Mechanism of Polyplex- and Lipoplex-Mediated Delivery of Nucleic Acids: Real-Time Visualization of Transient Membrane Destabilization without Endosomal Lysis

Zia ur Rehman, Dick Hoekstra, and Inge S. Zuhorn*

Department of Cell Biology, University Medical Center Groningen, University of Groningen, A. Deusinglaan 1, 9713 AV Groningen, The Netherlands

ABSTRACT Lipoplexes and polyplexes are widely applied as nonviral gene delivery carriers. Although their efficiencies of transfection are comparable, their mechanisms of delivery, specifically at the level of nucleic acid release from endosomes, are different. Thus, lipoplex-mediated release is proposed to rely on lipid mixing, as occurs between lipoplex and endosomal target membrane, the ensuing membrane destabilization leading to nucleic acid delivery into the cytosol. By contrast, the mechanism by which polyplexes, particularly those displaying a high proton buffering capacity, release their nucleic acid cargo from the endosome, is thought to rely on a so-called "proton sponge effect", in essence an osmotically induced rupturing of the endosomal membrane. However, although a wealth of indirect insight supports both these mechanisms, direct evidence is still lacking. Therefore, to further clarify these mechanisms, we have investigated the interaction of lipo- and polyplexes with HeLa cells by live cell imaging. As monitored over an incubation period of 2 h, our data reveal that in contrast to the involvement of numerous nanocarriers in case of lipoplex-mediated delivery, only a very limited number of polyplexes, that is, as few as one up to four/five nanocarriers per cell, with an average of one/two per cell, contribute to the release of nucleic acids from endosomes and their subsequent accumulation into the nucleus. Notably, in neither case complete rupture of endosomes nor release of intact polyplexes or lipoplexes into the cytosol was observed. Rather, at the time of endosomal escape both the polymer and its genetic payload are separately squirted into the cytoplasm, presumably *via* (a) local pore(s) within the endosomal membrane. Specifically, an almost instantaneous and complete discharge of nucleic acids and carrier (remnants) from the endosomes is observed. In case of lipoplexes, the data suggest the formation of multiple transient pores over time within the same endosomal membrane, *via* which the cargo is more gradually transferred into the cytosol.

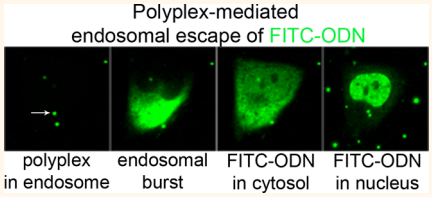

KEYWORDS: polyplexes · lipoplexes · endosomal escape · proton sponge effect · flip-flop mechanism · live cell imaging

Lipo- and polyplexes are promising nonviral tools for nucleic acid delivery into cells, for example, plasmids for transfection and siRNA for gene silencing.[1−4] To exert their function they have to cross several cellular barriers including the plasma and endosomal membranes and, in the case of plasmid or antisense oligonucleotide delivery, the nuclear membrane. Although each barrier represents a critical step in determining the final efficiency of nucleic acid delivery and effectivity of nucleic acid-based drugs, the release of genetic cargo from endosomes, that is, endosomal escape prior to their degradation in lysosomes, appears to be a major bottleneck. To release their cargo from endosomal compartments, lipo- and polyplexes are thought to employ different mechanisms, the molecular details of which are only gradually emerging.

Polyplexes, composed of polymers that display a high proton buffering capacity such as polyethyleneimine (PEI)[5,6] or polyamidoamine dendrimers (PAM),[7] carry titratable amines. In this manner, it has been proposed that such polymers can act as a so-called "proton sponge".[6,8] During endosome maturation, when the pH acidifies due to the activity of H-ATPase, the amines become protonated, while the excessive inflow of H^+ provokes the influx of Cl^- counterions for reasons of charge neutralization. It has thus been proposed that in order to compensate for an osmotic imbalance, subsequent water intake into the endosomes causes their osmotic swelling

* Address correspondence to i.zuhorn@umcg.nl.

Received for review October 24, 2012 and accepted April 18, 2013.

Published online April 18, 2013
10.1021/nn3049494

and eventual rupture, resulting in the release of polyplexes into the cytosol,[5,8] where subsequent dissociation of the nucleic acid cargo may occur.

Lipoplexes use a different mechanism to release their cargo into the cytosol that relies on lipid mixing, which may involve fusion and the formation of transient and local perturbations of the endosomal membrane through which nucleic acids can be released into the cytosol.[9,10] It has been proposed that the underlying mechanism is related to the inherent ability of the cationic lipids to engage, with or without helper lipids such as dioleoylphosphatidylethanolamine, in the formation of nonbilayer structures. Instrumental in the overall process is also the lipoplex-induced flip-flop of negatively charged phospholipids from the cytoplasmic to the inner face of the endosome,[11] forming charge neutral ion pairs with the cationic lipids,[12] thereby destabilizing the lamellar membrane organization and at the same time causing dissociation of the nucleic acids from the lipoplexes.

Although widely accepted, several reports have questioned the proton sponge mechanism,[13−15] largely because of a lack of direct evidence and because of entry of PEI complexes *via* a pathway (caveolae-mediated endocytosis) that may not rely on compartmental acidification.[16] An alternative escape mechanism, relying on membrane perturbation caused by a time-dependent increase of a protonation-induced tight apposition of the polyplex and endosomal membrane, has also been proposed. Strong circumstantial evidence in favor of the proton sponge effect was provided by Sonawane *et al.*,[17] showing the accumulation of Cl^- ions and swelling of the endosome in polyplex-mediated transfection. However, the individual fate of the polymer, its genetic cargo, and the endosome from where the release occurs, remain poorly addressed.[18,19] Obviously, microscopic imaging is a versatile tool to potentially obtain detailed insight into structural changes in the morphology of nanocarrier and endosomes which, by inference may lead to novel insight into the mechanism of nanocarrier-mediated gene delivery. Advanced electron microscopic technology may serve that purpose, although an approach that allows direct insight into the dynamics of the process is preferred. We therefore examined endosomal escape of nucleic acids as mediated by lipo- and polyplexes by live cell imaging of HeLa cells to further clarify the mechanism of nanocarrier-mediated delivery of nucleic acids, in particular, the polymer-based sponge effect. Our data support a highly effective discharge from endosomes following polyplex entry, but the observed effect, which can be described as "bursting" of the endosome, leads neither to complete endosomal lysis nor release of intact polyplexes into the cytosol. This implies that although seemingly fierce in nature, a yet relatively subtle mechanism underlies polyplex-mediated delivery.

TABLE 1. Physical Characterization (Size and Zeta Potential) of LPEI Polyplexes and LF2000 Lipoplexes Containing ODN and pDNA

	LPEI		LF2000	
	ODN	pDNA	ODN	pDNA
size (nm)	109.7 ± 36.6	90.9 ± 13.0	88.6 ± 1.1	487.2 ± 46.9
ζ potential (mV)	8.9 ± 0.8	5.1 ± 0.7	−5.7 ± 3.2	−25.8 ± 13.2

RESULTS AND DISCUSSION

PEI Polyplexes Induce Endosomal Bursting; Polyplex Dissociation Prior to Nucleic Acid Release. Previously, we demonstrated that PEI-mediated delivery of nucleic acids into HeLa cells occurs *via* the clathrin- and caveolae-mediated endocytic pathways.[20] To characterize this delivery process in further detail, an effort was undertaken to its visualization by live cell fluorescence imaging. Thus, HeLa cells were incubated with LPEI polyplexes containing FITC-labeled oligonucleotides (ODNs) and the interaction process was monitored in real time. As shown in Figure 1a and Movie 1a, near the cell surface and early after internalization, presumably by endocytosis, the polyplexes (physical characterization shown in Table 1) are visible as bright, globular fluorescent structures.

Approximately 30−35 min after addition of polyplexes, the dot-like appearance of the polyplexes quickly disappears over a time interval of less than 1 min, showing an initially *localized* "burst" of diffuse fluorescence that in the next 5−10 s starts to accumulate in the nucleus, reflected by the rapid distinction of the nuclear boundary in the cytoplasmic background. This process of nuclear accumulation of ODNs that occurs *via* passive diffusion[21] continues over at least 15−20 min (Figure.1a).

Although it is reasonable to assume that the observed burst(s) originate(s) from endosomal ODN release, this notion was supported by two pieces of evidence. First, when HeLa cells, prior to the addition of polyplexes, were incubated with Bafilomycin A1, which prevents endosome acidification, the release of fluorescently labeled ODNs was virtually completely inhibited (Figure 2a). In control cells, virtually all cells showed ODN-positive nuclei, while in BafA1-treated cells the ODNs remained localized within the endosomes in the cytoplasm of the cells (Figure 2b). Pretreatment of the cells with Bafilomycin A1 also inhibited the transfection efficiency with polyplexes to a similar extent (data not shown). In addition, the endosomes were labeled with Lysotracker-Red and cells were subsequently incubated with FITC-ODN-containing polyplexes. As can be seen in Figure 2c (and Supporting Information, Movie 2), polyplex-containing endosomes acidify while moving through the cytoplasm, which is evident from the recruitment of Lysotracker into these

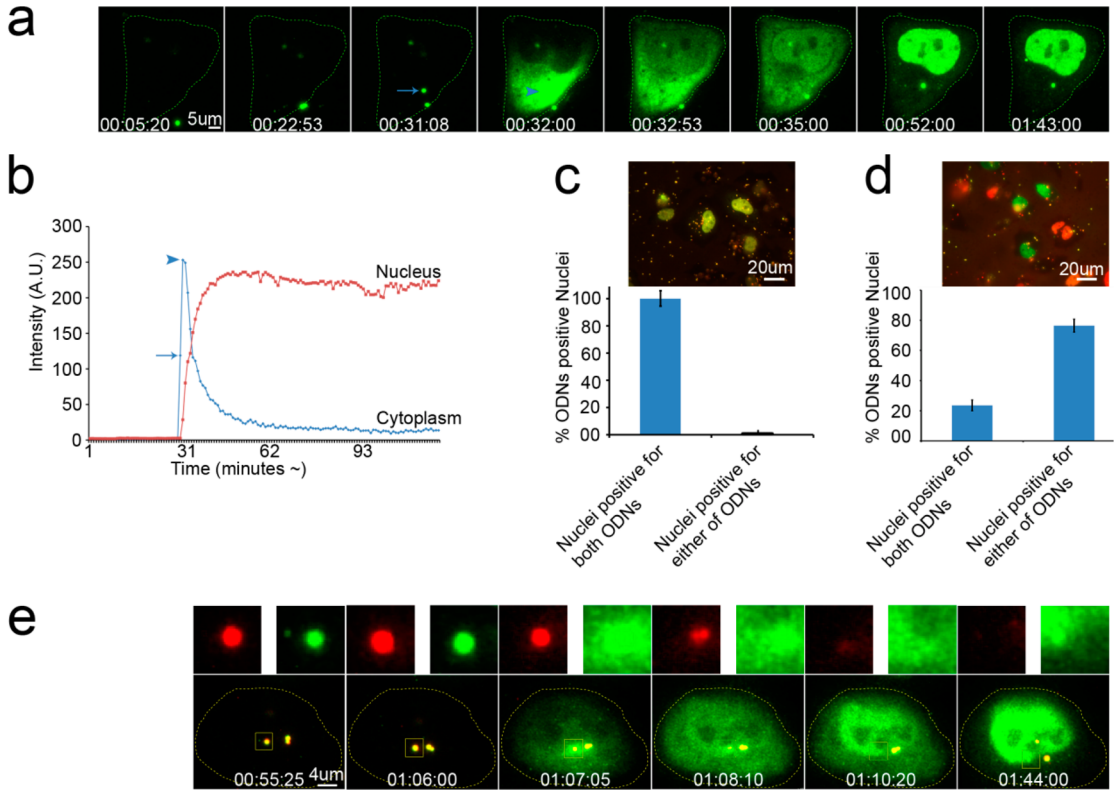

Figure 1. PEI-mediated cytosolic delivery of oligonucleotides occurs by endosomal bursting. HeLa cells were incubated with LPEI polyplexes containing FITC-labeled oligonucleotides (ODNs) and the interaction was monitored by live cell imaging (a). Selected frames from Movie 1a show that after internalization of the PEI polyplex (arrow in third panel), its ODN content is rapidly released into the cytoplasm (arrowhead in fourth panel), followed by a ready accumulation into the nucleus (panels 5−8). Line graph of Movie 1a showing the fluorescence at a region of interest (ROI) within the cytoplasm and within the nucleus at the time of the endosomal escape of ODNs, followed by their accumulation in the nucleus (b). The arrow indicates the fluorescence intensity of the ODNs within the endosome (*cf.* arrow in (a), panel 3), while the arrowhead indicates the cytoplasmic fluorescence intensity upon endosomal escape (*cf.* arrowhead in (a), panel 4). The dots in the graph correspond with the frames in Movie 1a, which are taken approximately every 52 s. HeLa cells were incubated with polyplexes carrying two different kinds of ODNs (FITC- and TAMRA-labeled) in a 1:1 molar ratio (c) or with a mixture of polyplexes, each carrying one of the labeled ODNs (d) for 2 h. Live cells were directly observed by fluorescence microscopy and the amount of nuclei that were positive for both ODNs or for one of the ODNs were quantified ($n = 3$, error bars represent standard deviation). Representative images are shown in the insets in c and d. (e) Polyplexes composed of FluoR-labeled LPEI (red) and FITC-ODNs (green) were incubated with HeLa cells, and monitored by live cell imaging. Representative frames from Movie 1b are shown, together with the signals (upper panels) from the individual fluorescence channels for the boxed area. The boxed area in (e) is yellow due to the colocalization of the PEI and ODN fluorescence (panels 1−4) and disappears in time due to loss of both signals after bursting (panels 5 and 6). Corresponding scale bars are shown in each figure. Time in (a) and (e) is indicated in hh/mm/ss.

compartments (Figure 2c, upper row). When the polyplex-containing endosome bursts, it releases both the ODNs and the Lysotracker (Figure 2c, last panel and also upper row). Accordingly, these data indicate that the observed bursts indeed reflect the release of ODNs from endosomal compartments, as delivered by the polyplexes.

To obtain further insight into the mechanism of polyplex-mediated delivery and the ensuing release of ODNs from endosomal compartments, the kinetics of the delivery event were monitored and quantified (Figure 1b) by fluorescence intensity measurements of a defined region of interest (ROI, selected based upon the size of polyplexes) in the cytoplasm (Figure 1a, third panel, arrow) and the nucleus of a cell. The initial steep increase in fluorescence intensity (up to a level indicated with an arrow in Figure 1b) of the cytoplasmic ROI (blue tracing) is due to the "capturing" of the labeled polyplex in the laser beam, following its internalization, and localization within an endosomal compartment. Next, a further increase in fluorescence intensity is seen (Figure 1b, arrowhead), which precedes a subsequent decrease in intensity. Likely, the latter increase corresponds to a relief of self-quenching of the polyplex-associated FITC-labeled ODNs at the time of endosomal escape, indicating their dissociation from the polyplex (arrowhead in graph 1b and Figure 1a, fourth panel), as reflected by a subsequent decrease of the (localized) fluorescence intensity of the cytoplasmic ROI spot, due to lateral diffusion of the labeled ODNs into the cytosol. Concomitantly, the fluorescence intensity measured in the nucleus rapidly increases, reflecting the passive diffusion of the relatively small (~20 bp) ODNs from the cytosol into the nucleus (graph 1b, red tracing; Figure 1a, panels 5−8). It is apparent from the data in Figure 1b that the

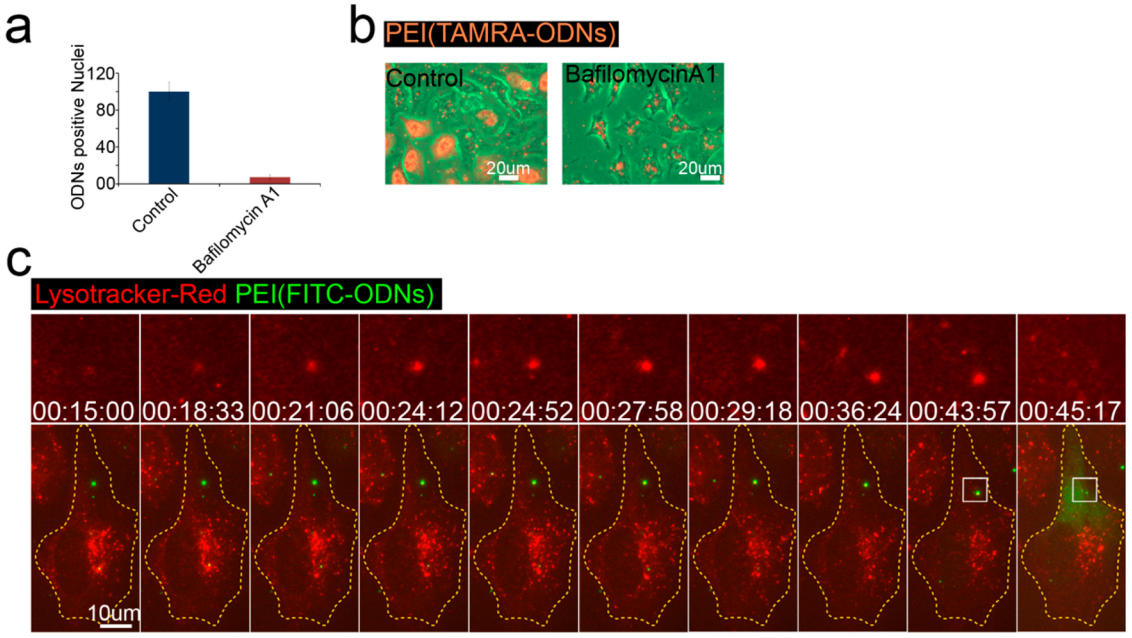

Figure 2. Acidification is required for PEI-mediated ODN release from endosomes. HeLa cells were incubated with or without Bafilomycin A1 for 30 min, followed by an incubation for 2 h with LPEI polyplexes carrying TAMRA-ODNs (a). Live cells were imaged by fluorescence microscopy and the amount of nuclei that were positive for ODNs were quantified using imageJ (n = 3, error bars represent standard deviation; control set at 100%). Representative images of both control and Bafilomycin A1-treated cells are shown (b). HeLa cells were labeled with Lysotracker-Red (red; see Materials and Methods) and subsequently incubated with polyplexes carrying FITC-ODNs (c). Selected frames (and individual red channel images of the cell area that contains a polyplex (green); upper panels) from Movie 2 show that endosomes gradually accumulate Lysotracker-Red (panels 1−9), which is released from the endosome upon its bursting, which is visualized by the cytoplasmic spread of the FITC-ODNs (last panel). Boxed areas in panels 9 and 10, indicate the location of the endosomal bursting. Scale bars are shown in each figure. Time in c is indicated in hh/mm/ss.

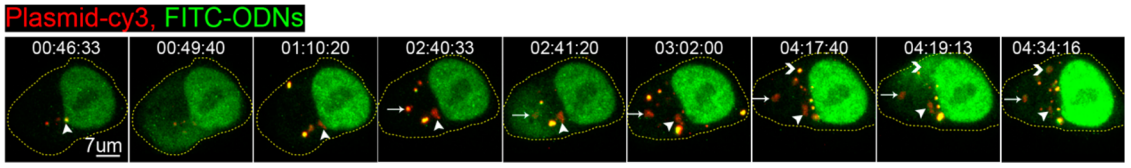

Figure 3. PEI-mediated cytosolic delivery of plasmid DNA occurs by endosomal bursting. A 1:1 weight ratio of Cy3-labeled pDNA (red) and FITC-ODNs (green) was mixed with unlabeled LPEI and added to HeLa cells. Selected frames from Movie 3a show that three polyplexes (yellow; arrowhead in panel 1, arrow in panel 4, and open arrowhead in panel 7) release their genetic payload into the cytosol. Subsequently, the ODNs (green) accumulate in the nucleus, whereas pDNA (red) remains in the cytosol. Representative size bar is shown in the first panel. Time is indicated in hh/mm/ss.

fluorescence intensity in the nucleus (red tracing) remains constant over >100 min, suggesting that during this time period there are no additional polyplexes that contribute to subsequent ODN delivery into the nucleus. Indeed, quite surprisingly, at the present conditions a very limited number of polyplexes appeared to contribute to the overall delivery process, which varied between one (Figure.1a) up to 4−5 bursts/cell, as shown in Figure 3.

To obtain additional support for this low frequency in delivery, HeLa cells were transfected with polyplexes carrying either a mixture of two differently labeled (red and green) ODNs in a 1:1 ratio or a mixture of two polyplex populations, each carrying one of the labeled ODNs. At the former conditions, essentially all cells showed yellow nuclei, following a 2 h incubation (Figure 1c), indicating the endosomal escape and subsequent nuclear accumulation of both green and red ODNs, which is not surprising since both ODNs are contained within one and the same polyplex. However, when the cells were incubated with a mixture of polyplexes containing either red or green ODNs, only 23% of the nuclei were yellow, while 77% were either green or red (Figure 1d). Similar results were obtained when the polyplexes contained plasmids (physical characterization shown in Table 1) instead of ODNs. Specifically, when the cells had been incubated for 2 h with polyplexes that carried pDNAs coding for GFP and RFP, the next day essentially all cells expressed both plasmids. However, when the plasmids were complexed separately with the polymers, and cells were transfected with a mixture of these polyplexes, the amount of cells coexpressing both plasmids drastically dropped while the majority

of the cells expressed only one of the plasmids (data not shown). These results provide further evidence that for polyplex-mediated nucleic acid delivery endosomal escape of nucleic acids, derived from delivery *via* a single polyplex, can be responsible for the final level of transfection efficiency. The extremely low delivery efficiency of polyplexes in terms of particle number was unexpected, and the underlying reason is unclear. Clearly, additional particles are internalized (Figure 1a, frames 5−8; Figure 1c,d fluorescence images) but they fail to discharge their contents and seemingly stable particles can be seen in the cytoplasm for several hours after their internalization. Clearly, size does not appear to be a governing parameter as endosomal escape occurs for both small and large polyplexes (data not shown).

The rapid dequenching of FITC-fluorescence at the time of endosomal escape of the ODNs, as indicated by the subsequent decrease of fluorescence (Figure.1b, blue tracing), might suggest that the dissociation of cargo and carrier occurs in the endosome. Therefore, the fate of the PEI polymer upon endosomal escape of the genetic cargo was examined next. In this case HeLa cells were incubated with double labeled polyplexes, that is, containing FluoR-labeled LPEI (red) and FITC-labeled oligonucleotides (green) and observed with live cell confocal microscopy (Supporting Information, Movie 2b). In the upper panels of Figure.1e the time-dependent appearance of the FITC-labeled ODN cargo (green) and polymer (red) are visualized in separate channels. Evidently, following the initial burst as reflected by the scattered diffuse distribution of the ODNs (3rd frame), the contours of the polymer carrier are still very similar as those of the original carrier (frames 1 and 2). Even after 1 min (frame 4), when the released ODNs localize to the cytoplasm and when accumulation in the nucleus becomes apparent, a clearly localized, although slightly deformed appearance of the carrier can still be discerned. Only over the next minutes (frames 5 and 6), the polymer carrier appears to fragment and the remnants subsequently disappear (frame 6). Accordingly, the data indicate that dissociation of the ODNs from the polyplex very likely occurs in the endosomal compartment, and that at least part of the carrier (remnants) remains associated with the compartment at a time when the ODNs have essentially been released into the cytosol and transported to the nucleus. Thus, these results are in marked contrast with what has been previously suggested, namely that polyplexes are released in an intact manner from endosomes following osmotic lysis, and that the release of their genetic payload occurs in the cytosol by exchange of polymers from the polyplexes with negatively charged cellular components.[22−24] Because these claims were largely based on delivery of plasmids, which are substantially larger in size than the ∼20 bp ODNs that were used here, we next investigated the endosomal escape of polyplexes carrying plasmid DNA (pDNA).

PEI-Mediated Cytosolic Delivery of Plasmid DNA Occurs in a Similar Way As Delivery of ODNs, but Plasmid DNA Does Not Move Freely in the Cytoplasm. To investigate whether mechanistic differences may exist between polymer-mediated release of relatively small (∼20 bp) ODNs *versus* large (4.7 kb) plasmids across the endosomal membrane, LPEI-polyplexes were prepared that contained both Cy3-labeled pDNA and FITC-labeled ODNs (red + green = yellow). The complexes were incubated with HeLa cells and polyplex-cell interaction was monitored by live cell imaging. At the time of endosomal escape, as revealed by the appearance of ODNs into the cytosol (Figure 3, second panel) and subsequent accumulation of nuclear fluorescence (Figure 3, third panel), the pDNA signal (Figure 3, arrowhead in the third and following panels) can be clearly discerned by its red Cy3-fluorescence after release of the FITC-labeled ODN. At the time of endosomal escape, a distinct increase in plasmid size becomes apparent, which presumably reflects pDNA decondensation following its dissociation from the polymer. However, in contrast to the mobility of ODNs, the plasmid remains localized at (Figure 3, frames 1−3) or near the site of release and fails to diffuse into the cytosol. Consistently, as shown in Figure 3 (see also Supporting Information, Movie 3a), three additional polyplexes consecutively release their content from the endosomes in which they are contained, leading to a proportional increase in nuclear fluorescence intensity, but the released plasmids remain very closely localized to the site of release (Figure 3, arrow and arrow heads). This is in agreement with previous observations showing that large DNA fragments like pDNA are poorly, if at all, mobile in the cytoplasm.[21] In addition, dissociation of the PEI/pDNA complex is reminiscent of that of the PEI/ODN polyplex, eventually resulting in PEI dispersal throughout the cell's cytoplasm (Supporting Information, Movie 3b; *cf.* Figure 1b).

Endosomes Are Not Lysed upon Polyplex-Mediated Release of Nucleic Acids. So far the data indicate that upon endosomal bursting, the polyplex cargo is efficiently released into the cytosol, with a concomitant escape of the polymer, that is, intact polyplexes were not seen to be released from endosomes. This would suggest that the sponge effect, proposed to involve osmotic swelling and subsequent lysis[5,6,17] might not be as destructive as thought to the integrity of the endosomal membrane. Thus, rather than complete lysis, our data as obtained in the present study would be compatible to a more subtle process, involving a degree of membrane rupture that precludes the integral release of polyplexes from endosomes. To obtain experimental support for such a scenario, we investigated the endosomal integrity in the process of polyplex-induced bursting, employing various membrane

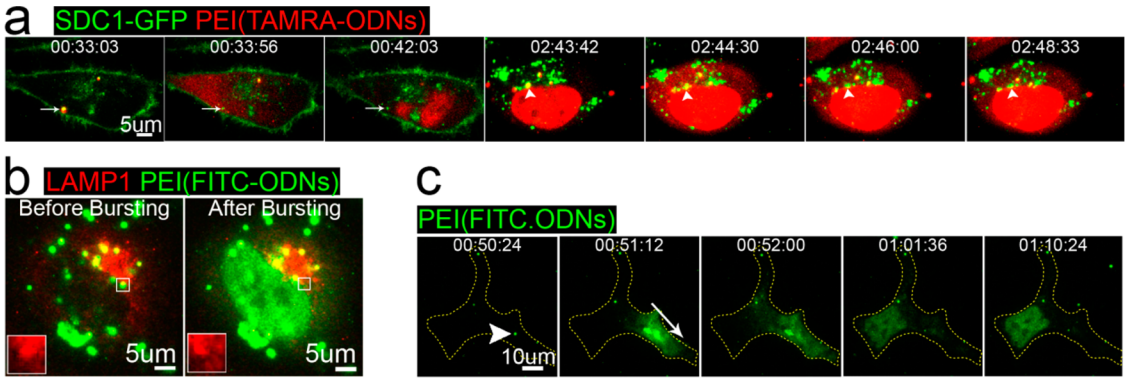

Figure 4. ODN release does not lead to the complete rupture of the endosome. (a) HeLa cells expressing GFP-labeled syndecan-1 (SDC1-GFP; green; see Materials and Methods) were incubated with LPEI polyplexes carrying TAMRA-ODNs (red) and visualized by live cell confocal microscopy. Selected frames from Movie 4a show that endosomal bursting takes place from SDC1-positive compartments (arrow in panels 1−3; arrowhead in panels 4−7). The ODNs accumulate in the nucleus, leaving behind SDC1-positive vesicles (arrow in panels 2 and 3; arrowhead in panels 6 and 7). (b) Two frames are selected from live cell imaging in which a polyplex-containing endosome, positively stained for LAMP1, bursts, resulting in the release of ODNs and their accumulation into the nucleus, leaving behind the LAMP1 positive compartment. Insets show the magnified area where bursting takes place, showing the presence of the LAMP1 positive vesicle. (c) Selected frames from Movie 4b show that bursting of a polyplex-containing endosome (arrowhead in panel 1) does not result in a randomized radial spread of ODNs, but rather shows a vectorial release of ODNs toward the lower right corner of the cell (indicated with arrow in panel 2). Subsequently, the ODNs distribute throughout the cytoplasm (panel 3) and accumulate in the nucleus (panels 4 and 5). Time is indicated in hh/mm/ss.

markers that were monitored by live cell imaging. To this end, HeLa cells were used that express syndecan 1-GFP (SDC1-GFP), a transmembrane receptor for polyplexes that mediates their internalization by endocytosis.[25−27] As shown in Figure 4a, panels 1−3 (see also Supporting Information, Movie 4a), the SDC1-GFP expressing cells reveal a somewhat fuzzy plasma membrane staining, reflecting syndecan distribution in the plasma membrane and extensions protruding from it, presumably filopodia and other filaments.[27] Upon addition of polyplexes, containing TAMRA-labeled ODNs, polyplex binding induces clustering of the syndecans, a necessary step for polyplex internalization, as was shown previously.[25,26] Indeed, in panel 1 of Figure 4a, two polyplexes carrying TAMRA-labeled ODNs can be seen, colocalizing with SDC1 as reflected by the yellow colocalization signal. Actual internalization of the polyplexes is supported by the observation that one of the polyplexes (indicated with arrow in panels 1−3 in Figure 4a) releases its content into the cytosol, leading to accumulation of the released ODNs (red) in the nucleus. At the very site of release, a bright green spot is left behind of which it is then reasonable to assume that it represents the SDC1-positive endosome from which the nucleic acid (red) was liberated. In time, a second endosomal escape occurs in the same cell as visualized in panels 4−7 (arrowhead), resulting in an additional increase in the nuclear ODN signal, while again leaving behind an endosomal compartment, brightly labeled by green SDC1-GFP fluorescence Supporting Information, Movie 4a). Very similar results were obtained in HeLa cells expressing LAMP1-RFP, a late endosomal/lysosomal marker. When the cells were incubated with polyplexes carrying FITC-ODNs, the nucleic acids were released and accumulated in the nucleus, whereas the LAMP1-positive compartments still localized to the site of release (Figure 4b). Together, these data thus support the notion that polyplex-mediated delivery, relying on a proton sponge effect, does not lead to a complete lysis of the endosome and scattering of endosomal remnants into the cytosol.

Consistent with this notion is the observation that instead of a randomized diffusion of ODNs into the cytosol upon their release from the endosome, they seem to be vectorially jetted into the cytoplasm, that is, it is tempting to suggest that the release appears to occur from one particular region of the endosomal membrane and has a directional nature. In Movie 4b and its corresponding still images in Figure 4c, it can be seen that upon endosomal escape the ODNs first move to the lower right corner of the cell (arrow) and then flow back upward to where the nucleus is located. This finding does not support the occurrence of a complete rupture of endosomes, in line with the observations that syndecan- or LAMP1-labeled endosomes can be clearly discerned in the cytosol after endosomal discharge of polyplex-delivered nucleic acids. Accordingly, we propose a model in which protonation causes the highly charged polyplex to firmly and intimately interact with the inner surface of the endosome, where a very local osmotic or mechanical effect, aided by the increase in membrane tension due to the osmotic swelling of the endosome, may lead to a local rupture of the endosomal membrane. The fast kinetics of ODN release from endosomes, as shown in Movie 4b (*cf.* Movie 1a), is best explained by a prior pressure buildup within the endosome, forcefully driving out

the rapidly diffusing ODNs, through polyplex-membrane interaction-induced local membrane perturbations or pores. We do not exclude that, depending on the number of such polyplexes within an endosome, such events could lead to the complete rupture of the compartment and the release of polyplexes as such. However, neither complete lysis nor release of intact polyplexes was observed in the present study. Nevertheless, the relative rapid discharge of the nucleic acid cargo from the endosomal compartment is compatible with a mechanism involving a substantial local permeation of the endosomal membrane which facilitates the fast release of the cargo, that is, within seconds after the onset of the observed "bursting" (*cf.* Figure 1a). In passing, we also note that not only the polyplex cargo is released but also other endosomal contents may apparently leak out following the bursting event, as reflected by the disappearance of Lysotracker from the compartments (Figure 2c).

In the case of lipoplex-mediated delivery, the endosomal membrane is thought to be similarly perturbed, which, however, relates to a mixing of cationic and endosomal membrane lipids, including negatively charged phospholipids like phosphatidylserine. The latter's interaction with the cationic lipid will cause dissociation of the nucleic acid from the carrier and, concomitantly, due to a so-called ion-pairing effect[9,10,12] promote the formation of nonbilayer structures, which will destabilize the endosomal membrane and allows the release of the nucleic acid. *A priori*, one might thus envision a more gentle release of cargo from lipoplexes than the more forceful osmotically driven discharge from endosomes observed in case of polyplexes with high buffering capacity. It was therefore of interest to similarly examine the mode of lipoplex-mediated delivery.

Lipoplex-Mediated Release of ODNs Is More Gradual than That Observed for Polyplexes. To visualize in real time the delivery and release of nucleic acids, as mediated by lipoplexes, HeLa cells were incubated with LF2000 lipoplexes containing FITC-ODNs (physical characterization shown in Table 1), and their interaction was monitored by live cell fluorescence imaging. Compared to polyplex-mediated delivery, two distinctions became immediately apparent. First, lipoplex-mediated delivery, reflected by the onset of visible accumulation of fluorescently tagged ODNs in the nuclei, appeared to occur much faster (within 5 min, Figure 5a, Supporting Information, Movie 5a) than polyplex-mediated delivery (approximately 30−60 min after the onset of incubation, Figures 1e and 2c). Second, the typical bursting process, seen for polyplexes, was not observed for lipoplex-mediated delivery, and the actual release had to be largely inferred from the accumulation of the ODNs in the nucleus. Thus, as anticipated, the kinetics of ODN release from lipoplexes *versus* polyplexes per se were grossly different. As shown in Figure 5a and Movie 5a, the nuclear fluorescence of the accumulating ODNs gradually intensifies, as supported by quantitatively monitoring of the nuclear fluorescence (Figure 5b, blue tracing), indicating a gradual, stepwise increase of ODN release. Given the fast accumulation of ODN in the nucleus once released from the endosome, the data thus suggest that their dissociation from the lipoplexes and subsequent release across the endosomal membrane represents a more gradual event than that observed in case of release following polyplex-mediated delivery (*cf.* Figure 1a). Indeed, when tracking individual lipoplex-containing endosomes (Figure 5a, arrow in panels 1−4 and arrowhead in panels 5−8) the diminishment in fluorescence, presumably reflecting the release of ODNs into the cytosol, is an equally gradual process (green and red tracings in Figure 5b).

To obtain further insight into the mechanism of lipoplex-mediated delivery, we next investigated the fate of the cationic lipid at the time of endosomal escape of the ODNs. To this end, the lipoplexes were labeled with rhodamine-labeled PE (red) and FITC-labeled ODNs (green) and the interaction of thus labeled complexes with HeLa cells was monitored by live cell fluorescence imaging. As illustrated in Figure 5c (and Supporting Information, Movie 5b), following internalization in endosomes, the colabeled lipoplexes are clearly discernible as bright yellow dots, resulting from the colocalization of the red rhodamine-labeled lipid and the green FITC-labeled ODNs. As a function of time, all dots gradually turn red, as they release their green ODNs into the cytosol which rapidly accumulate into the nucleus (see also Figure 5c). Accordingly, these data indicate that the lipid carrier remains associated with the endosome and does not accompany the released genetic cargo. This is different from the polymer content of polyplexes, which is expelled into the cytoplasm together with the genetic payload.

In addition, our data suggest that relative to the very limited number of polyplexes engaged in delivery, the number of lipoplexes that deliver their contents is substantially higher. To further support this notion, HeLa cells were incubated with lipoplexes that contain both TAMRA- and FITC-ODNs in a 1:1 ratio. At these conditions, it was observed that essentially all cells contained both labels in their nuclei, as reflected by the yellow fluorescence, arising from the colocalized red TAMRA- and green FITC-labeled ODN (Figure 5d, *cf.* Figure 1c). When cells were incubated with a 1:1 mixture of lipoplexes that contained either TAMRA or FITC ODNs, more than 80% of the cells similarly showed nuclei positive for both ODNs (Figure 5e), implying that both labeled populations discharged their cargo, which subsequently colocalized in the nucleus. Because polyplex-mediated delivery resulted in label colocalization in approximately 20% of the

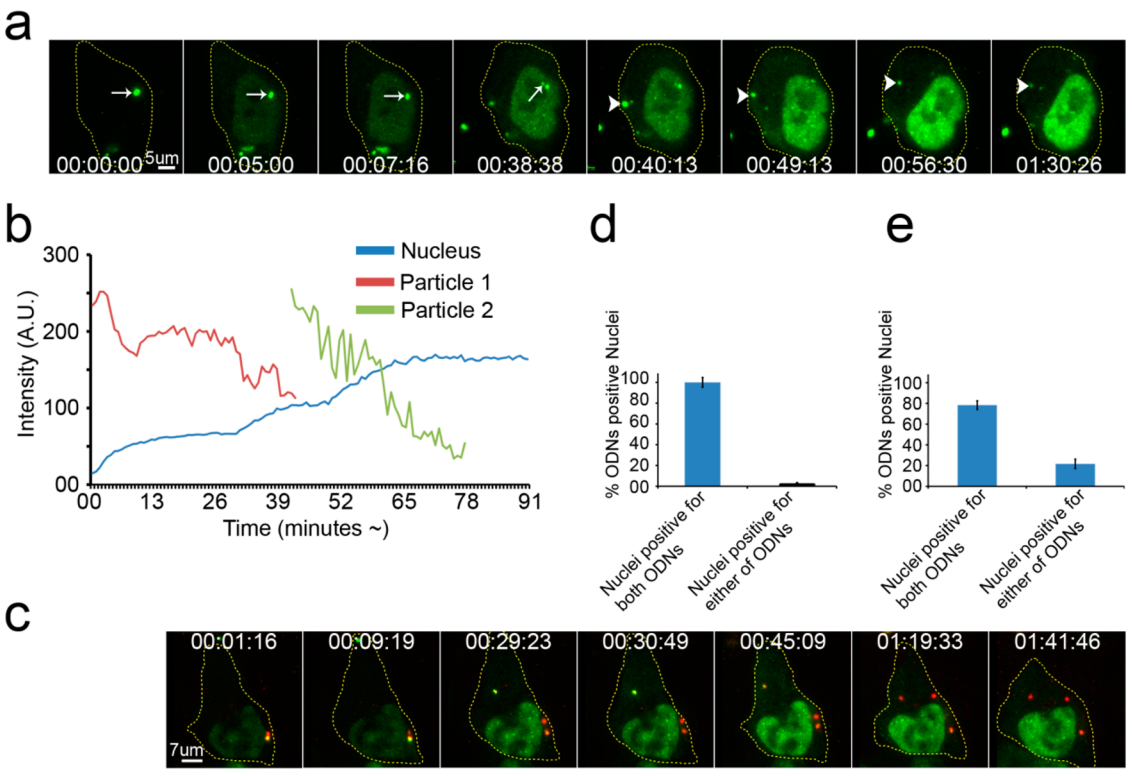

Figure 5. LF2000 lipoplexes show a gradual release of their genetic payload into the cytosol. (a) HeLa cells were incubated with LF2000 lipoplexes carrying FITC-ODNs and monitored by live cell confocal microscopy. Selected frames from Movie 5a show two lipoplexes (arrow in panels 1−4 and arrowhead in panels 5−8) that successively release parts of the ODN content, revealing a stepwise decrease in ODN fluorescence within the endosome, and a concomitant increase in ODN fluorescence within the nucleus. (b) Line graph of (a), showing the gradual nature of the endosomal escape of genetic cargo from lipoplexes, which contrasts the burst release following polyplex-mediated delivery (compare Figure 1b). The two lipoplexes (red and green lines) slowly lose their contents, which corresponds with a steady increase in the nuclear fluorescence signal (blue line). (c) Rhodamine-labeled LF2000 (red) was complexed with FITC-ODNs (green) and added to HeLa cells. Selected frames from Movie 5b show that three lipoplex-containing endosomes that initially appear yellow (due to colocalization of carrier (red) and contents (green)) gradually turn red while releasing ODNs into the cytoplasm. (d, e) HeLa cells were incubated for 2 h with lipoplexes carrying two different kinds of ODNs (FITC- and TAMRA-labeled) in a 1:1 molar ratio (d) or with a mixture of lipoplexes each carrying one of the labeled ODNs (e). Live cells were directly observed by fluorescence microscopy and the amount of nuclei that were positive for both ODNs or for one of the ODNs were quantified (n = 3, error bars indicate standard deviation). At both conditions most of the cells are positive for both of the ODNs. Time in (a) and (c) is indicated in hh/mm/ss.

cells (Figure 1d), this indicates that lipoplex-mediated delivery involves release of contents from multiple carriers.

CONCLUSIONS

Live cell imaging allows for the study of highly dynamic cellular processes, including the endosomal processing of poly- and lipoplexes, by the use of fluorescent proteins and synthetic fluorophores. To capture these dynamic processes high imaging rates are needed to obtain high spatial and temporal resolution. Many imaging methods that enable high spatial resolution such as single point laser scanning confocal microscopy require high illumination intensities. These high intensities are not compatible with long-term live-cell imaging experiments, because they induce cellular phototoxicity.

Here we used spinning disk confocal microscopy, which is emerging as the technique of choice for investigation of dynamics in living cells, to capture the event of endosomal escape of poly- and lipoplexes. With spinning disk confocal microscopy high imaging rates with adequate contrast and minimal photobleaching can be obtained at low levels of illumination, that is, preventing cellular phototoxicity.

In the present work we have presented direct evidence in support of the proton sponge effect, instrumental in the mechanism of nucleic acid delivery by highly buffering polyplexes, like those based on PEI. Interestingly, we observed a release of the nucleic acids without endosomal lysis, from LPEI polyplexes in HeLa cells. The precise nature of this release, that is, in a random or vectorial manner, evidently requires further work, and its understanding will further contribute to unraveling details of the underlying mechanism of polyplex-endosomal membrane interaction. A quantitative analysis of the endosomal release of nucleic acids would be desirable. As a minimum requirement this would only be possible if an appropriate fluorescent label (*i.e.*, that remains detectable at and after "bursting" conditions) for marking the endosome is included and if higher imaging rates can be

applied without inducing cellular phototoxicity. For that reason, fluorophores or fluorescent proteins that emit in the yellow, orange, and red regions of the spectrum can be used in order to minimize damage to cells by short wavelength illumination.

Most remarkable, only a limited number of polyplexes appear to participate in the process of nucleic acid delivery, ranging from 1 up to 5 per cell. The kinetics of release indicates the nucleic acids to be released as an almost instantaneous event, while whole polyplexes were not observed to appear in the cytosol. In contrast, the release observed in case of lipoplex-mediated delivery revealed a sustainable-like mechanism of release proceeding over an extended time interval. Apart from the evident distinction in kinetics of ODN release from endosomes, when comparing lipoplex- *versus* polyplex-mediated delivery, reflecting clear differences in the underlying mechanisms of release, the images as presented in Figure 5a,b make it tempting to speculate on the mechanism of lipoplex-mediated release. Indeed, the more gradual "leakage-like" or sustained release of ODNs when delivered by lipoplexes suggests a more subtle destabilization of the endosomal membrane according to a pore forming mechanism, rather than a fusion mechanism that is thought to result in a more instantaneous mode of contents release. Evidently, further work will be needed to clarify this issue.

As discussed in a previous paragraph, our data suggest that a local destabilization of the endosomal membrane, possibly induced by an osmotic/mechanical effect at the site of tight charge-driven polyplex-endosomal membrane interaction, may underlie the mechanism of polyplex-mediated delivery. In contrast, a more subtle destabilization of the endosomal membrane relying on its perturbation by nonbilayer structures appears to be the driving force in lipoplex-mediated release, its more gradual kinetics (compare Figure 5b, blue tracing, *vs* Figure 1b, red tracing) indicating that multiple pores over time are required to completely discharge the nucleic acid content. Consistent with the latter notion is the observation that the lipids remained associated with the endosome. In this context, we have previously shown that membrane pores induced by plasma membrane-inserted-cationic lipid have a restricted lifetime (10−15 min, depending on their size),[28] before lateral randomization of the membrane destabilizing cationic lipids reseals the induced pore. Accordingly, prolonged release over a period of almost 1 h would suggest that multiple pores of a transient lifetime are formed in the endosomal membranes, which may thus account for a gradual release until complete discharge of the cargo has occurred into the cytosol.

Finally, in contrast to the relative rapid onset of ODN release from lipolexes, ODN release from polyplexes became apparent after approximately 30 min, following internalization. This may suggest that for polyplexes the site of ODN entry takes place from late, more strongly acidified endosomes, possibly reflecting the strength of the osmotic gradient required, in conjunction with the ensuing tightening of charge-driven polymer-endosomal membrane interaction, for eventual (local) destabilization of the membrane. However, given the perinuclear region where release occurs and given a fairly minimal delivery efficiency in terms of number of polyplexes that are effectively delivering their contents, this localization may be favorable for plasmid delivery, plasmids being substantially less motile than ODNs in the cytosol. Clearly, these and other issues, including the reason why such a limited number of polyplexes release their contents, as shown in this study, warrant further studies.

MATERIALS AND METHODS

Reagents. Lipofectamine 2000 was purchased from Invitrogen. Both unlabeled linear polyethyleneimine (LPEI, average MW = 22 kDa) and fluorescently labeled LPEI (jetPEI-FluoR) were obtained from PolyPlus-transfection (Illkirch, France). Fluorescently labeled plasmids were from Mirus (Mirus M.A) and fully phosphorothioated FITC- and TAMRA-labeled oligonucleotides were obtained from Biognostik (Gottingen, Germany) and Biomers.net, respectively. (FITC-5′-ACTACGACCTACGTGAC-3′; TAMRA-5′-ACTACTACACTAGACTAC-3′)

Cells. HeLa cells were obtained from ATCC and maintained in 25 cm^2 flasks in DMEM/F-12 (Dulbecco's modified Eagle medium F-12, Gibco, The Netherlands) at 37 °C and 5% CO_2. The medium was supplemented with 2 mM L-glutamine (Gibco, The Netherlands), 100 units/mL each penicillin, streptomycin (Invitrogen), and 10% (v/v) FCS.

Plasmids. pEGFP-N1 was obtained from Clontech (U.S.A.), Syndecan-1 (pSDC1-GFP), and LAMP1-RFP were kindly provided by Dr. Yves Durocher (National Research Council (NRC), Canada) and Dr. Walther Mothes (Yale University, CT, U.S.A.), respectively. All plasmids were amplified from E.Coli using GenElute HP Plasmid Mini/Midiprep kits (Sigma-Aldrich), using the manufacturer's protocol.

Preparation of Lipo- and Polyplexes, Transfection, and ODN Delivery. For the expression of SDC1-GFP and LAMP1-RFP, HeLa cells were plated in glass-bottomed, two-well chambers (Lab-Tek Chambered Coverglass, Thermo Fisher Scientific, Denmark) at 1.8×10^5 cells/well, two days prior to the experiment. After 24 h, the cells were washed once with serum-free medium and transfected with plasmid using Lipofectamine 2000, according to the manufacturer's protocol.

For preparation of lipoplexes, 3 μL of lipofectamine 2000, and 1 μg of plasmid DNA or 0.1 nmol of ODN were diluted in 100 μL of HBSS, after which the nucleic acid solution was added to the lipid solution and incubated for 20 min at room temperature prior to the addition to cells. For preparation of polyplexes (N/P 5), 2 μL of LPEI and 1 μg of plasmid DNA or 0.1 nmol of ODN were diluted in 100 μL of HBSS, after which the polymer solution was added to the nucleic acid solution, and incubated for 20 min at room temperature prior to the addition to cells.

For measurement of transfection efficiency of LPEI polyplexes cells were plated in twelve wells plates at 1.5×10^5 cells/well, one day before the experiment. After 24 h, the cells were washed twice with serum-free medium and then incubated with polyplexes, suspended in HBSS, carrying 1 μg of pEGFP-N1

at N/P 5. (for data on particle size and zeta potential, see ref 20) After 2 h of incubation, the cells were washed and complete cell culture medium was added, with an additional medium change after 24 h. Transfection efficiency was measured after 48 h by FACS analysis (Elite, Coulter 10000 events λ_{ex} 488 nm/λ_{em} 530 nm). When inhibitors were employed, the cells were preincubated with the indicated inhibitors for 30 min, and subsequently, polyplexes were added, with inhibitors kept present.

For live cell imaging and fluorescence microscopy, lipoplexes, and polyplexes were used, containing fluorescently labeled ODNs. When required, the polyplexes contained FluoR-labeled LPEI, and lipoplexes contained rhodamine-labeled lipofectamine 2000 (0.5 mol % of Rhodamine-PE (Avanti Polar Lipids Inc., U.S.A.) inserted *via* ethanol injection method). A total of 0.1 nmol FITC or TAMRA-labeled oligonucleotides (ODNs) or 1 μg Cy-labeled plasmid (Mirus MA) was complexed with LF2000 (3 μg; conditions according to manufacturer's instruction) or PEI polyplexes (2 μL; at an N/P ratio of 5.0).

Particle Size and Zeta Potential Measurements. LPEI polyplexes and LF2000 lipoplexes, containing 5 μg plasmid DNA or 0.5 nmol of ODN, were prepared in 1 mL of MQ water or 10 mM NaCl for size and zeta potential measurement, respectively. Measurements were performed on a Zetasizer Nano (Malvern Instruments Ltd.)

Fluorescence Microscopy. Fluorescence microscopy (Olympus) was used to quantitatively measure the release of oligonucleotides per cell. Briefly, one day before the experiment, HeLa cells were plated at 1.5×10^5 cells/well in 12-well plates. After 24 h, the cells were washed twice with serum-free medium. Lipo/polyplexes, containing 0.1 nmol of oligonucleotides, were mixed in 200 μL of HBSS, added to the cells and incubated for 2 h. Subsequently, the cells were washed once with HBSS and live cells were directly placed on glass slides, carrying a drop of HBSS, and investigated by fluorescence microscopy. In the presence of Bafilomycin A1, the cells were preincubated with the inhibitor for 30 min and, subsequently, the lipo/polyplexes were added with the inhibitor present. Images were analyzed using ImageJ software (NIH). For each condition, the ODN-positive nuclei were counted in 100−150 cells in ~10 random fields of view and expressed as percentage of total number of nuclei. Experiments were repeated three times (n = 3).

Live Cell Imaging Using Spinning Disk Confocal Microscopy. For live cell imaging, cells were plated on special glass-bottomed, two-well plates (Lab-TekTM Chambered Coverglass, Thermo Fisher Scientific, Denmark). In case cells were employed expressing SDC1-GFP or LAMP1-RFP, the cells were plated two days before the experiment at 1.8×10^5 cells/well. Subsequently, the cells were transfected with either SDC1 or LAMP1 plasmid using Lipofectamine 2000 according to the manufacturer's protocol. On the day of the experiment, cells expressing either of the plasmid were placed in a Solamere Spinning Disk Confocal Microscope (based on a Leica DM IRE2 inverted microscope, Leica Microsystem, Germany, Solamere, Salt Lake City, U.S.A.) equipped with a temperature/CO_2-controlled cabinet and automated stage. Cells that express LAMP1-RFP or SDC1-GFP were selected before addition of polyplexes. Image acquisition was directly started after addition of the polyplexes using InVivo software (Media Cybernetics, Inc., Bethesda, MD). Images were further analyzed using ImageJ (NIH) and Imaris software (Bitplane AG, Switzerland). When similar experiments were carried out with cells that did not express the above-mentioned plasmids, the cells were plated at 3×10^5 cells/well one day before the experiment. Otherwise, incubation conditions and data acquisition were identical to those described for the LAMP1 and SDC1 expressing cells.

Conflict of Interest: The authors declare no competing financial interest.

Acknowledgment. Microscopy imaging was performed at the UMCG Imaging Center (UMIC), supported by The Netherlands Organisation for Health Research and Development (ZonMW Grant 40-00506-98-9021).

Supporting Information Available: Nine supporting videos. This material is available free of charge *via* the Internet at http://pubs.acs.org.

REFERENCES AND NOTES

1. Semple, S. C.; Akinc, A.; Chen, J.; Sandhu, A. P.; Mui, B. L.; Cho, C. K.; Sah, D. W.; Stebbing, D.; Crosley, E. J.; Yaworski, E.; et al. Rational Design of Cationic Lipids for siRNA Delivery. *Nat. Biotechnol.* **2010**, *28*, 172–176.
2. Guo, X.; Huang, L. Recent Advances in Nonviral Vectors for Gene Delivery. *Acc. Chem. Res.* **2012**, *45*, 971–979.
3. Nguyen, J.; Szoka, F. C. Nucleic Acid Delivery: the Missing Pieces of the Puzzle?. *Acc. Chem. Res.* **2012**, *45*, 1153–1162.
4. Eliyahu, H.; Barenholz, Y.; Domb, A. J. Polymers for DNA Delivery. *Molecules* **2005**, *10*, 34–64.
5. Boussif, O.; Lezoualc'h, F.; Zanta, M. A.; Mergny, M. D.; Scherman, D.; Demeneix, B.; Behr, J. P. A Versatile Vector for Gene and Oligonucleotide Transfer into Cells in Culture and *In Vivo*: Polyethylenimine. *Proc. Natl. Acad. Sci. U.S.A.* **1995**, *92*, 7297–7301.
6. Behr, J. The Proton Sponge: a Trick to Enter Cells the Viruses Did Not Exploit. *Chimia* **1997**, *51*, 34–36.
7. Tang, M. X.; Redemann, C. T.; Szoka, F. C., Jr *In Vitro* Gene Delivery by Degraded Polyamidoamine Dendrimers. *Bioconjugate Chem.* **1996**, *7*, 703–714.
8. Behr, J. P. Synthetic Gene Transfer Vectors II: Back to the Future. *Acc. Chem. Res.* **2012**, *45*, 980–984.
9. Wasungu, L.; Hoekstra, D. Cationic Lipids, Lipoplexes and Intracellular Delivery of Genes. *J. Controlled Release* **2006**, *116*, 255–264.
10. Hafez, I. M.; Maurer, N.; Cullis, P. R. On the Mechanism Whereby Cationic Lipids Promote Intracellular Delivery of Polynucleic Acids. *Gene Ther.* **2001**, *8*, 1188–1196.
11. Xu, Y.; Szoka, F. C., Jr. Mechanism of DNA Release from Cationic Liposome/DNA Complexes Used in Cell Transfection. *Biochemistry* **1996**, *35*, 5616–5623.
12. Lewis, R. N.; McElhaney, R. N. Surface Charge Markedly Attenuates the Nonlamellar Phase-Forming Propensities of Lipid Bilayer Membranes: Calorimetric and (31)P-Nuclear Magnetic Resonance Studies of Mixtures of Cationic, Anionic, and Zwitterionic Lipids. *Biophys. J.* **2000**, *79*, 1455–1464.
13. Godbey, W. T.; Wu, K. K.; Mikos, A. G. Tracking the Intracellular Path of Poly(ethylenimine)/DNA Complexes for Gene Delivery. *Proc. Natl. Acad. Sci. U.S.A.* **1999**, *96*, 5177–5181.
14. Funhoff, A. M.; van Nostrum, C. F.; Koning, G. A.; Schuurmans-Nieuwenbroek, N. M.; Crommelin, D. J.; Hennink, W. E. Endosomal Escape of Polymeric Gene Delivery Complexes Is Not Always Enhanced by Polymers Buffering at Low pH. *Biomacromolecules* **2004**, *5*, 32–39.
15. Benjaminsen, R. V.; Mattebjerg, M. A.; Henriksen, J. R.; Moghimi, S. M.; Andresen, T. L. The Possible "Proton Sponge" Effect of Polyethyleneimine (PEI) Does Not Include Change in Lysosomal pH. *Mol. Ther.* **2012**, *21*, 149–157.
16. Rejman, J.; Conese, M.; Hoekstra, D. Gene Transfer by Means of Lipo- and Polyplexes: Role of Clathrin and Caveolae-Mediated Endocytosis. *J. Liposome Res.* **2006**, *16*, 237–247.
17. Sonawane, N. D.; Szoka, F. C., Jr; Verkman, A. S. Chloride Accumulation and Swelling in Endosomes Enhances DNA Transfer by Polyamine−DNA Polyplexes. *J. Biol. Chem.* **2003**, *278*, 44826–44831.
18. Pichon, C.; Billiet, L.; Midoux, P. Chemical Vectors for Gene Delivery: Uptake and Intracellular Trafficking. *Curr. Opin. Biotechnol.* **2010**, *21*, 640–645.
19. Conese, M.; Biffi, A.; Dina, G.; Marziliano, N.; Villa, A. Comparison between Cationic Polymer and Lipid in Plasmidic DNA Delivery to the Cell Nucleus. *Open Gene Ther. J.* **2009**, *2*, 21–28.
20. ur Rehman, Z.; Hoekstra, D.; Zuhorn, I. S. Protein Kinase A Inhibition Modulates the Intracellular Routing of Gene Delivery Vehicles in HeLa Cells, Leading to Productive Transfection. *J. Controlled Release* **2011**, *156*, 76–84.
21. Lukacs, G. L.; Haggie, P.; Seksek, O.; Lechardeur, D.; Freedman, N.; Verkman, A. S.; Size-Dependent, D. N. A. Mobility in Cytoplasm and Nucleus. *J. Biol. Chem.* **2000**, *275*, 1625–1629.

22. Akinc, A.; Thomas, M.; Klibanov, A. M.; Langer, R. Exploring Polyethylenimine-Mediated DNA Transfection and the Proton Sponge Hypothesis. *J. Gene Med.* **2005**, *7*, 657–663.
23. Cho, Y. W.; Kim, J. D.; Park, K. Polycation Gene Delivery Systems: Escape from Endosomes to Cytosol. *J. Pharm. Pharmacol.* **2003**, *55*, 721–734.
24. Pollard, H.; Remy, J. S.; Loussouarn, G.; Demolombe, S.; Behr, J. P.; Escande, D. Polyethylenimine but Not Cationic Lipids Promotes Transgene Delivery to the Nucleus in Mammalian Cells. *J. Biol. Chem.* **1998**, *273*, 7507–7511.
25. Paris, S.; Burlacu, A.; Durocher, Y. Opposing Roles of Syndecan-1 and Syndecan-2 in Polyethyleneimine-Mediated Gene Delivery. *J. Biol. Chem.* **2008**, *283*, 7697–7704.
26. Kopatz, I.; Remy, J. S.; Behr, J. P. A Model for Non-Viral Gene Delivery: Through Syndecan Adhesion Molecules and Powered by Actin. *J. Gene Med.* **2004**, *6*, 769–776.
27. Rehman, Z. U.; Sjollema, K. A.; Kuipers, J.; Hoekstra, D.; Zuhorn, I. S. Nonviral Gene Delivery Vectors Use Syndecan-Dependent Transport Mechanisms in Filopodia to Reach the Cell Surface. *ACS Nano* **2012**, *6*, 7521–7532.
28. Oberle, V.; Bakowsky, U.; Zuhorn, I. S.; Hoekstra, D. Lipoplex Formation under Equilibrium Conditions Reveals a Three-Step Mechanism. *Biophys. J.* **2000**, *79*, 1447–1454.